

Quantifying bioirrigation in aquatic sediments: An inverse modeling approach

*Christof Meile*¹

Utrecht University, Faculty of Earth Sciences, P.O. Box 80021, 3508 TA Utrecht, The Netherlands

*Carla M. Koretsky*²

Georgia Institute of Technology, School of Earth & Atmospheric Sciences, Atlanta, Georgia 30332-0340

Philippe Van Cappellen

Utrecht University, Faculty of Earth Sciences, P.O. Box 80021, 3508 TA Utrecht, The Netherlands

Abstract

An inverse model was developed to quantify the depth distributions of bioirrigation intensities in sediments based on measured solute concentration and reaction rate profiles. The model computes statistically optimal bioirrigation coefficient profiles; that is, profiles that best represent measured data with the least number of adjustable parameters. A parameter reduction routine weighs the goodness-of-fit of calculated concentration profiles against the number of adjustable parameters by performing statistical *F*-tests, whereas Monte Carlo simulations reduce the effects of spatial correlation and help avoid local minima encountered by the downhill simplex optimization algorithm. A quality function allows identification of depth intervals where bioirrigation coefficients are not well constrained. The inverse model was applied to four different depositional environments (Sapelo Island, Georgia; Buzzards Bay, Massachusetts; Washington Shelf; Svalbard, Norway) using total CO₂ production, sulfate reduction, and ²²²Rn/²²⁶Ra disequilibrium data. Calculated bioirrigation coefficients generally decreased rapidly as a function of depth, but distinct subsurface maxima were observed for sites in Buzzards Bay and along the Washington Shelf. Irrigation fluxes of O₂ computed with the model-derived bioirrigation coefficients were in good agreement with those obtained by difference between total benthic O₂ fluxes measured with benthic chambers and diffusive fluxes calculated from O₂ microprofiles.

Biogeochemical cycles in aquatic sediments depend on coupled reaction and transport processes. The latter include diffusion, advection, and biologically induced transport. Benthic macrofaunal activity may enhance solute transport through the passive or active flushing of infaunal burrow networks with water originating from the sediment–water interface (bioirrigation). In sediments with dense macrofaunal populations, bioirrigation may increase solute exchange fluxes across the sediment–water interface to such an extent that measured benthic fluxes are due primarily to bioirrigation rather than diffusion (e.g., Hammond and Fuller 1979; Archer and Devol 1992). In heavily bioturbated sediments, enhanced biological transport may increase the return of nutrients to the overlying water. Such benthic nutrient release promotes benthic–pelagic coupling and contributes to the high primary productivity of nearshore marine environments (Rowe et al. 1975).

Bioirrigation also has a significant effect on the spatial distribution of early diagenetic processes in aquatic sedi-

ments. Flushing of burrow networks removes metabolites and reduced species from the bulk pore waters. At the same time, the introduction of oxidants via burrows to depths at which bulk conditions are highly reducing promotes reoxidation reactions near burrow walls (Aller and Aller 1998). Zonation in sediment redox conditions near burrow walls may affect the microbial ecology at depth significantly by increasing the variety of potential microbial niches (Aller et al. 1983; Mayer et al. 1995; Lowe et al. 2000). In addition, if solute transport rates are rapid relative to reaction rates, as is often the case in sediments with intense bioirrigation, it may become difficult to infer dominant microbial organic carbon degradation pathways directly from pore water concentration gradients (e.g., Berner 1985; Fossing et al. 2000; Furukawa et al. 2000).

In this study, an inverse model is used to estimate the magnitude and the depth dependence of bioirrigation in aquatic sediments from measured concentration and reaction rate profiles. Bioirrigation has been represented previously in early diagenetic models as a nonlocal transport process, in which the bioirrigation intensity with depth is quantified by a mass transfer, or bioirrigation, coefficient (Boudreau 1984; Emerson et al. 1984). In contrast to previous studies (e.g., Martin and Sayles 1987), the inverse approach presented here does not require an a priori, and hence subjective, assignment of the functional depth dependence of the bioirrigation coefficient profile. The inverse approach is also advantageous because measurement uncertainties can be accounted for explicitly in the model calculations, thus limiting the overinterpretation of measured data. Furthermore, con-

¹ Corresponding author (meile@geo.uu.nl).

² Present address: Western Michigan University, Department of Geosciences, Kalamazoo, Michigan 49008.

Acknowledgments

We thank J. Kostka for providing sulfate reduction rate measurements from the Sapelo Island salt marsh site in advance of publication. We thank E. Viollier, K. Hunter, and S. Joye for valuable discussions.

This work was supported financially by the Office of Naval Research (grant N00014-98-1-0203).

straints may be applied to parameter values, allowing knowledge regarding the system to be incorporated into the model.

The procedure presented in this study is similar to that of Berg et al. (1998), who used an inverse approach to identify reaction rate profiles in sediments with known transport rates. In particular, our model shares a similar (but not identical) approach with respect to the reduction of adjustable parameters, which leads to a statistically optimal description of bioirrigation as a function of depth. However, the work presented here differs significantly from that of Berg et al. (1998) in a number of ways. First, Berg et al. (1998) used the inverse approach to solve for reaction rate profiles, whereas in this study the focus is on quantifying biologically induced solute transport. Second, the procedure presented here explicitly accounts for measurement uncertainties, and it allows model results to be constrained using a priori information about bioirrigation intensities in a given environment. Third, our model includes Monte Carlo simulations, in order to address shortcomings of the optimization and parameter reduction algorithms. In particular, a quality function is developed that identifies depth regions where the procedure does not lead to meaningful results. Finally, with the model presented, bioirrigation coefficient profiles can be determined from simultaneous analysis of multiple chemical constituents.

Model development

Early diagenetic equation and boundary conditions—Biologically induced solute exchange, or bioirrigation, can be incorporated into the general early diagenetic equation of a solute species by combining it with terms representing diffusion, advection, and reaction.

$$\frac{\partial(\phi C)}{\partial t} = \frac{\partial}{\partial z} \left(D \phi \left(\frac{\partial C}{\partial z} \right) \right) - \frac{\partial(v\phi C)}{\partial z} + \alpha \phi (C_{\text{flush}} - C) + R \quad (1)$$

D is the diffusion coefficient of the solute species corrected for tortuosity, temperature, salinity, and pressure (Ullman and Aller 1982), v is the advection velocity relative to the sediment–water interface (neglecting $\phi C(\partial\omega/\partial z)$, where ω is the burial velocity), R is the net rate of production of the solute at depth z , α is the bioirrigation coefficient (in units of inverse time), ϕ is the porosity, C is the solute concentration in the bulk sediment, and C_{flush} is the flushing concentration of the solute, generally approximated as the concentration in the bottom water. Use of the relatively simple, nonlocal formulation of bioirrigation given in Eq. 1 is justified by its structural similarity to a general exchange function approach (Boudreau 1987) and its mathematical equivalence to a 3-D description of continuously flushed vertical tube-shaped burrows (Aller 1980; Boudreau 1984).

Equation 1 is solved numerically at steady state using a blended finite difference scheme (Fiadeiro and Veronis 1977; Boudreau 1997). In advection-dominated systems, this blended scheme becomes a backward difference formula, whereas in diffusion-dominated systems, it becomes a central difference scheme, thus balancing stability and accuracy of the numerical scheme. Discretization transforms the bioirrigation coefficient profile $\alpha(z)$ into a step function $\alpha(i)$, and therefore α values for each depth segment are required.

Several options for defining upper and lower boundary conditions are included in the model. Fixed concentration or constant flux boundaries may be assigned, or mass balance considerations may be used to determine the solute concentration at either the upper or lower boundary. In the mass balance approach, the consumption or production of the solute species is integrated between the upper and lower boundary and combined with the calculated fluxes of the species into or out of the sediment via diffusion and bioirrigation. The solute concentration in either the top or bottom depth segment is then adjusted until mass balance is satisfied. In all of the simulations described below, the option of fixed concentrations is used for both the upper and lower boundary conditions.

Inverse optimization routine—Using measured concentration and reaction rate profiles at steady state, it is possible to solve the discretized form of Eq. 1 directly for the bioirrigation coefficient profile. However, this type of approach often yields oscillating values of $\alpha(z)$, as described for reaction rate profiles by Berg et al. (1998). In addition, the direct method does not allow bioirrigation coefficients to be constrained to physically meaningful values. For example, negative values of the mass transfer coefficient α are not physically reasonable, but often result from a simple forward application of Eq. 1. In addition to eliminating physically unreasonable solutions, the inverse approach also allows uncertainties and constraints to be incorporated directly into the model, and it does not require an arbitrary choice for the depth dependence of the bioirrigation coefficients.

In the algorithm developed in this study (Fig. 1), an initial guess of the bioirrigation coefficient depth profile is systematically altered using a modified downhill simplex method (Press et al. 1989) to find a profile that reproduces measured concentration profiles within specified limits of uncertainty. The downhill simplex algorithm is an iterative procedure to minimize an objective function that reflects the quality of a calculated solution. The iterative optimization of the objective function is repeated until convergence between the calculated and measured concentration profiles, within a given uncertainty, is achieved at all depths or until a specified number of iterations (typically >1,000) are completed.

The objective function (OF) accounts for the fit to the data, via the sum of the weighted least square differences between the measured and calculated concentrations at each depth in the profile, modified by penalty functions. The latter increase the value of the objective function when values of $\alpha(i)$ either violate the parameter constraints or result in calculated concentrations that are less than a defined limiting value (typically 0). Mathematically,

The objective function (OF) accounts for the fit to the data, via the sum of the weighted least square differences between the measured and calculated concentrations at each depth in the profile, modified by penalty functions. The latter increase the value of the objective function when values of $\alpha(i)$ either violate the parameter constraints or result in calculated concentrations that are less than a defined limiting value (typically 0). Mathematically,

$$\text{OF} = \sum_{i=1}^n \left(\frac{C_{\text{meas},i} - C_{\text{calc},i}}{\sigma_{C,i}} \right)^2 + t \sum_{i=1}^n \left(\frac{C(\alpha_{\text{lim}})_{\text{calc},i} - C_{\text{calc},i}}{\sigma_{C,i}} \right)^2 + c \sum_{i=1}^n \left(\frac{C_{\text{lim},i} - C_{\text{calc},i}}{\sigma_{C,i}} \right)^2, \quad (2)$$

where $\sigma_{C,i}$ is the uncertainty of the measured concentration

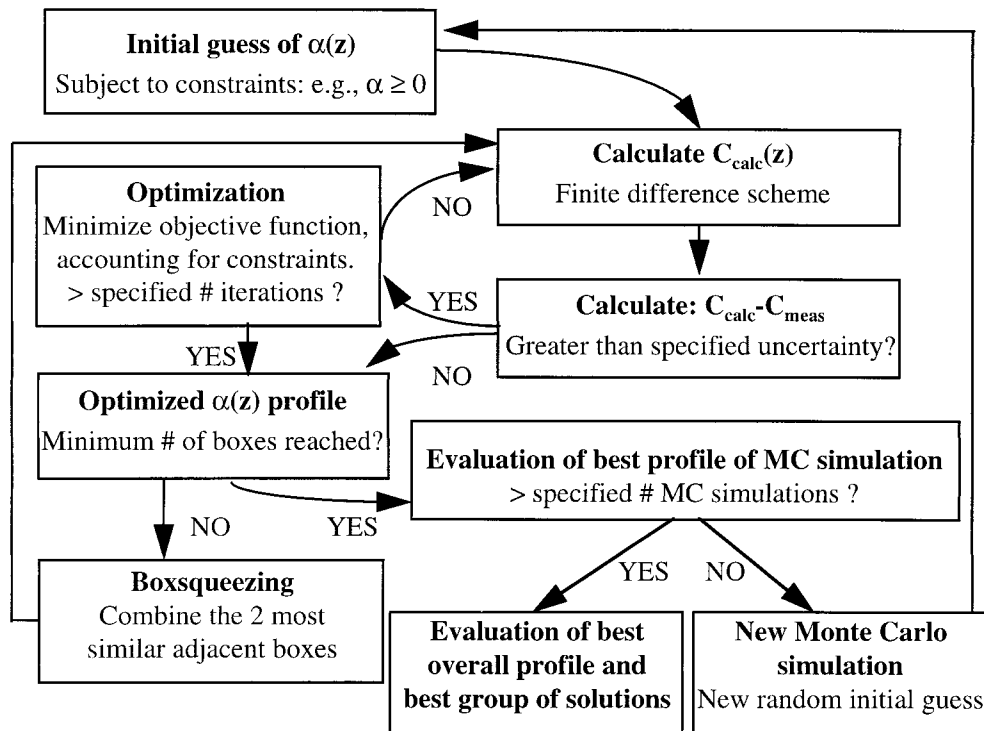


Fig. 1. Flowchart of the inverse modeling approach.

and n is the number of depth segments, chosen to reflect the resolution of the measurements. The weighting parameters, t and c , are set to 0 if no violations of the constraints on parameters or concentrations occur; otherwise, they are assigned values ≥ 0 . In the simulations shown here, t and c are both set to 10 when violations occur, but other values can be assigned by the user if necessary. C_{meas} , C_{calc} , and C_{lim} are the measured, calculated, and limit concentrations (e.g., $C_{\text{lim}} = 0$; forcing modeled concentrations to values ≥ 0), respectively; $C(\alpha_{\text{lim}})$ is the concentration calculated using the constraining value of α (e.g., $\alpha_{\text{lim}} = 0$) at the depths where α violates the constraints.

Reduction of independent parameters and statistical quality of fit—The optimization procedure described above leads to a solution that is consistent with both the measured data and the applied constraints. However, adjacent depth segments may have very similar bioirrigation coefficient values, so that the profile could be simplified (i.e., the number of fitting parameters reduced) without a significant loss in the quality of the fit between the measured and calculated concentration profiles. Therefore, a “boxsqueezing” algorithm was developed to systematically reduce the number of fitting parameters. In this algorithm, the depth discretization of the profile is changed by combining the two adjacent depth segments with the most similar parameter values into a single segment. After the two segments are “squeezed” together, the optimization routine is repeated using the new discretization. This process is continued until a prespecified minimum number of parameters is reached.

The statistically optimal depth discretization is determined using two criteria. The primary criterion is that the calcu-

lated concentration at each depth in the initial discretization must lie within the uncertainty of the measured data (i.e., convergence is required at each depth). If more than one discretization of the parameter profile meets this criterion, then the quality of the fit associated with each discretization is weighted against the simplicity of the bioirrigation coefficient profile by performing a series of F -tests at a 95% confidence level (for details on the test statistics, see Kleinbaum et al. 1988; Berg et al. 1998). In this way, the boxsqueezing routine allows the objective determination of the simplest parameter profile that describes the measured data.

Monte Carlo simulations—The most severe limitation of the downhill simplex algorithm used to optimize the parameter profile is that it may yield solutions associated with a local, rather than global, minimum of the objective function. Therefore, in the presence of local minima, the optimized parameter value depends on the initial guess of that value. This limitation of the downhill simplex optimization method is overcome by performing a series of Monte Carlo simulations with initial guesses of the parameter profile chosen at random from a specified range of values. In the model presented here, the range of initial parameter values at each depth may either be specified explicitly or may be constrained by calculating, at each depth, the maximum and minimum parameter value (subject to specified constraints), which yields a calculated concentration consistent with the measured concentration and its associated uncertainty. Each Monte Carlo simulation yields a single, statistically optimal parameter profile based on the criteria described in the previous section.

Optimized profiles resulting from the individual Monte

Carlo simulations are compared and ranked according to the same criteria used to determine the best discretization of the parameter profile. Ranks are first assigned to profiles based on convergence. That is, profiles with greater numbers of converged depths (using the original depth discretization) are ranked above profiles with fewer converged depths. Within a group of profiles with the same number of converged segments, each profile is rated as better or worse than each of the other profiles. For two profiles with different numbers of adjustable parameters, this rating is based on an *F*-test, which determines whether the additional adjustable parameters significantly improve the fit of the calculated concentration profiles to the measured ones. For two profiles with the same number of adjustable parameters, the profile with the lower objective function value receives the higher ranking. The overall rank of a given profile is then based on the number of times it ranked better than other profiles in the pool. This procedure leads to the selection of the “best” individual bioirrigation coefficient profile.

In the parameter reduction scheme used in this study, the combination of depth segments is nonreversible. Thus, if depth segments are combined in a way that does not correctly reflect the underlying process, subsequent optimization of the profile will be biased. However, inappropriate combination of two depth segments as an artifact of the optimization routine will likely result in a profile ranked lower than others produced by the Monte Carlo simulations. This is because it will either result in a worse fit or it will prevent the further reduction of the numbers of adjustable parameters because the convergence criterion cannot be met.

The variability of the bioirrigation coefficient profiles produced by the Monte Carlo simulations serves as a qualitative indicator of how well the α values can be constrained at any given depth. Part of the variability, however, results from spatial correlation, that is, coupling between adjacent spatial nodes. Because diffusion tends to smooth concentration profiles, an overprediction of the “true” (unknown) irrigation coefficient coupled to an underpredicted value in an adjacent depth segment may yield a good fit to the measured data. Decreasing the number of adjustable parameters generally lessens spatial coupling by broadening the depth segments with constant parameter values. However, if α changes significantly over a small depth interval, the parameter reduction may instead induce spatial coupling. The effects of spatial coupling are greatly reduced by averaging results from multiple Monte Carlo simulations. Thus, the average irrigation coefficient profile calculated from the individual parameter profiles of the Monte Carlo simulations may lead to a solution closer to the true value of α (see the Model performance section). However, care must be taken to include in the averaging only those solutions that belong to the global minimum. Based on test runs with model scenarios (see below), it was found that between 100 and 500 Monte Carlo simulations were sufficient to obtain reproducible results.

Quality function—To assess the quality of the model results, a quantitative quality measure (Q) was developed, which reflects the sensitivity of the concentration profile to changes in the parameter profile (i.e., the irrigation coefficient), as well as on the goodness of the fit between the

measured and calculated concentration profiles. It is defined, at any given depth z , as

$$Q = \left| S \cdot \frac{\alpha_{\text{avg}}}{\Delta C} \right|, \quad (3)$$

where ΔC , the difference between measured and calculated concentrations at depth z , accounts for the goodness of fit. The sensitivity (S) is evaluated by perturbing the optimized α profile at depth z while leaving the rest of the profile unchanged. The value of S is then equal to the difference in concentration between the optimized and perturbed α profile at depth z , divided by the difference in the optimized and perturbed value of α at this depth. Multiplication by a scaling factor α_{avg} , the average value of the bioirrigation coefficient over the entire core depth, results in a dimensionless value of Q . This allows comparison of the quality of model results for environments with different bioirrigation intensities.

The limit value of Q , below which model results become meaningless, was established empirically by applying the model to a number of synthetic scenarios with known bioirrigation coefficient profiles (see the section Model performance). In Fig. 2, deviations between calculated and imposed irrigation coefficients from a variety of model scenarios are plotted against Q_{min} , the lowest value of $Q(z)$ over the whole depth profile. The absolute deviation of α at the depth where Q equals Q_{min} and the relative error at this depth both increase significantly below a value of $Q_{\text{min}} \sim 0.4$. The largest absolute error in α was generally found at the depth where Q equals Q_{min} . In what follows, the bioirrigation coefficient is deemed well constrained for depth intervals where $Q \geq 0.4$.

To increase computational efficiency, the quality function is only evaluated for the statistically best Monte Carlo simulation profile and for a limited number of averaged profiles. To select the profiles to be averaged, the statistically best profiles from the individual Monte Carlo simulations are ranked as described in the previous section. Averaged profiles are then calculated from these profiles, using those with a rank better than 1, 2, 5, 10, 25, 50, and 100% of the total number of Monte Carlo simulations. Of these averaged profiles, that which produced the highest value of Q_{min} is taken as the best representation of $\alpha(z)$. The selected individual profiles are used to calculate standard deviations about the best estimate of $\alpha(z)$.

Nonunique nature of solutions—It is sometimes assumed (erroneously) that models that provide a good fit to measured data are “correct.” In fact, for natural systems, the available quality or quantity of data often cannot provide unique solutions to modeled problems. In other words, model solutions may yield an excellent fit to measured data without correctly representing the underlying process(es). For example, it may not be possible to determine unique values of α with Eq. 1, particularly when the flushing concentration lies within the uncertainty of the measured pore water concentrations. In such a case, high values of α simply shift the calculated concentration closer toward the value of the flushing concentration. Thus, an irrigation coefficient profile

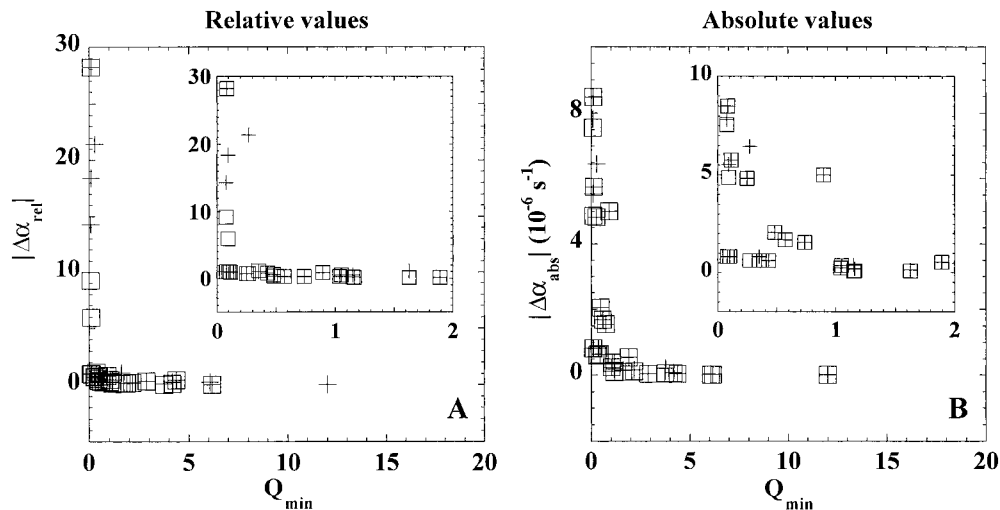


Fig. 2. Magnitudes of (A) relative and (B) absolute deviations between calculated and “true” irrigation coefficients plotted against the minimum value of the quality function for the entire depth profile. Data are from a variety of synthetic model simulations (see text). Open squares represent the error at the depth at which Q reaches its minimum value; crosses depict the maximum error in the entire profile. See text for detailed discussion.

might be found that reproduces measured concentrations, but that does not accurately represent the in situ exchange intensity.

To minimize such problems, α is extrapolated from adjacent depth segments if (1) the flushing concentration lies within the uncertainty of the measured value and the calculated concentration is closer to the flushing concentration than to the measured concentration (indicating a likely overestimate of α) or (2) the flushing concentration is very close to the calculated concentration (difference smaller than 10% of the uncertainty at that depth), and the corresponding irrigation coefficient is very large (e.g., $>10^{-3} \text{ s}^{-1}$). In the top and bottom depth segments, where fixed concentration boundary conditions apply, α is undefined and is therefore set equal to the value in the adjacent depth segment.

Multicomponent optimization—A more robust quantification of solute exchange may be obtained by using independent data sets for multiple chemical constituents. Such an approach assumes that the same irrigation coefficient applies to the different constituents. This is likely to hold true if the solute species have similar physicochemical properties or if the frequency of burrow flushing is slow enough to allow equilibration of the chemical composition of pore waters and burrow solution (Hammond et al. 1985). In the case of continuous flushing of burrows, however, α is related both to the diffusion coefficient and the diffusive path length (Boudreau 1984). The latter is influenced by the reactivity of a chemical (Marinelli and Boudreau 1996); hence, differences in irrigation coefficients may be expected for different chemical species.

In a multicomponent calculation, the objective function (OF) should reflect all the constituents involved in the calculation of α . Thus, it is defined as the sum of the contributions from the different chemical constituents. In the multicomponent simulations shown below, the objective

function was modified slightly so that only depth segments lacking convergence contributed to the value of OF. This leads to stronger dependence on convergence than for the standard definition of OF given by Eq. 2. Irrigation coefficient profiles are ranked according to the same criteria as in the one-component case. However, the quality of fit is determined separately for each concentration profile, and the sum of ranks from this evaluation is used as the decision variable for the overall quality of an irrigation coefficient profile. $Q(z)$ is assigned the average value of all profiles at a given depth. Hence, high values of $Q(z)$ indicate that the irrigation coefficient is well defined by all of the chemical species used in the calculation. Values of Q are likely to be lower in the multicomponent approach, however, because the resulting bioirrigation coefficient profile must provide a good fit to all species involved in the optimization.

Model performance

Before the model was applied to data from natural systems, it was first tested using a series of simulations designed to analyze the performance of the three primary model components: the downhill simplex optimization, the reduction of adjustable parameters (boxsqueezing), and the Monte Carlo simulations. The finite difference scheme has been thoroughly tested previously (Meile 1999).

A set of synthetic rate and irrigation coefficient profiles was used with specified fixed concentration boundary conditions in order to calculate corresponding concentration profiles. From these rate and concentration profiles, with uncertainties specified for each concentration, the irrigation coefficient profiles were back-calculated with the inverse model. In this way, model performance was assessed for a variety of hypothetical environmental scenarios.

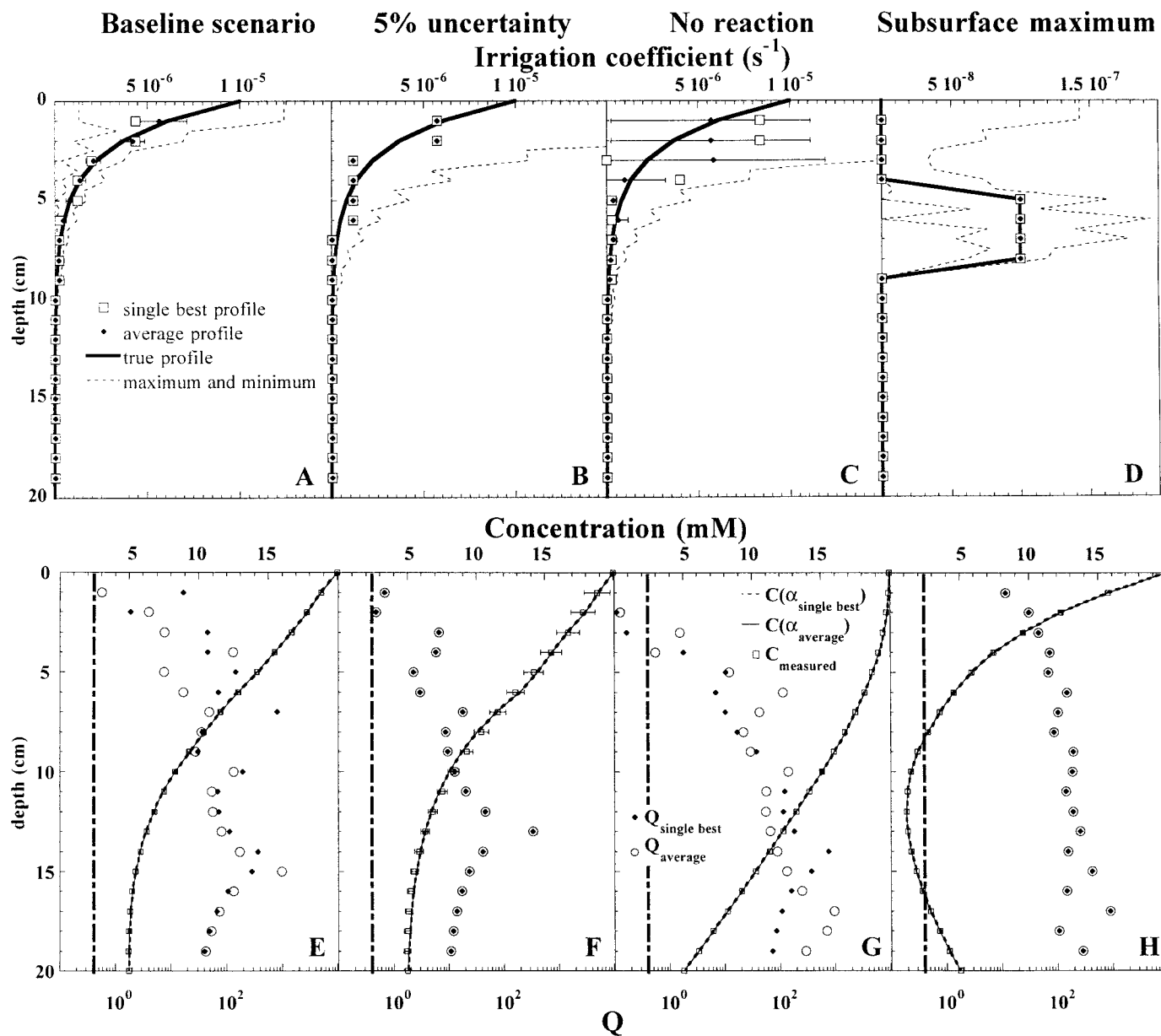


Fig. 3. Model results using imposed depth profiles of rate and bioirrigation coefficient. (A) Single best and averaged irrigation coefficient profiles and minimum and maximum values of α for all converged simulations in the “baseline scenario,” which is defined by an exponentially decreasing solute consumption rate (R [mM s^{-1}] = $10^{-5} \exp(-15 \cdot z$ [cm]), a steeply decreasing bioirrigation coefficient profile, a 1% uncertainty in the concentrations, and fixed concentration boundary conditions. (B) Symbols and simulations are identical to (A) except that the uncertainties on concentrations are assigned a value of 5%. (C) Same as (A), except that the reaction rate is set to 0 at all depth. (D) Same as (A), except that the bioirrigation depth dependency is defined by a step function. (E)–(H) Concentration and quality function profiles for the simulations described in panels (A)–(D), respectively. The vertical dashed line shows the limit value of $Q = 0.4$, below which model results are no longer well constrained.

Model scenarios—Model performance is illustrated in Fig. 3. The baseline scenario is representative of a highly productive coastal–estuarine environment, with the rate and concentration profile corresponding to, for example, profiles of the net rate of sulfate reduction and the sulfate concentration.

The calculated profiles shown in Fig. 3A demonstrate that both the single, statistically best profile and the average profile reproduce the true bioirrigation coefficient profile very

well at most depths. The single best profile, however, fails to reproduce some of the fine structure of the true bioirrigation coefficient profile. In particular, the high value of α is underestimated at the 1-cm depth. Simplification of the modeled profiles through boxsqueezing (from 19 initial to five final depth segments) of the statistically best profile prevents the steep decrease of the true bioirrigation coefficients at the top of the profile from being simulated exactly (Fig. 3A). The lower values of the quality function near the top

Table 1. Study sites, input data, and summary of model results. The irrigation transfer velocity (V) is calculated by integrating the bioirrigation coefficient over the whole core depth; z_{90} is the depth at which the depth-integrated bioirrigation coefficient reaches 90% of the total transfer velocity. DIC is the concentration of dissolved inorganic carbon, R_{CO_2} is the DIC production rate, and SRR is the sulfate reduction rate.

Site	Water depth (m)	Data used	V (cm yr ⁻¹)	z_{90} (cm)
Malangen (Sv-1: 69°29.4'N 18°07.5'W)	329	DIC, pH, R_{CO_2}	4,267±982	14.5
Storefjorden (Sv-5: 77°33.0'N 19°05.0'W)	175	DIC, pH, R_{CO_2}	1,742±300	14.5
Sapelo Is. (Jun, 31°22'N 81°14'W)	intertidal	SO_4^{2-} , SRR	1,841±349	4
Sapelo Is. (Aug, 31°22'N 81°14'W)	intertidal	SO_4^{2-} , SRR	29,127±28,479	4
Buzzards Bay (near Weepecket Is.)	15	Rn/Ra	138	18
Washington Shelf, core 2A (MSSD-1, Aug)	86	SO_4^{2-} , SRR	341	28.5
		Rn/Ra	1,708±88	23.5
		Rn/Ra and SO_4^{2-} , SRR	959±446	23.5
Washington Shelf, core 3A (MSSD-2, Aug)	86	SO_4^{2-} , SRR	1,607±828	24.5
		Rn/Ra	898±200	21.5
		Rn/Ra and SO_4^{2-} , SRR	809±172	24.5

of the profile (Fig. 3E) reflect the lower sensitivity just below the water–sediment interface, which is due to the small value of the bioirrigation driving force ($C_{\text{flush}} - C[z]$).

Simulation results shown in Fig. 3B,F were calculated using the same reaction rate and bioirrigation profiles as in the baseline scenario, but the uncertainty associated with the measured concentration profile was increased from 1 to 5%. Due to the larger uncertainties, the number of depth segments with distinct values of α is reduced to just three in the statistically best irrigation coefficient profile. Although the calculated bioirrigation coefficient profile matches the imposed solution quite well, the range of possible α profiles leading to converged concentration profiles is considerably larger than for the case above. The maximum value increases to as much as 10^{-4} s^{-1} near the sediment–water interface. Thus, as expected, the quality of the model results is directly influenced by the quality of the data.

Results shown in Fig. 3C were calculated using the baseline scenario, but with an imposed solute consumption rate equal to zero, as would be the case for an unreactive species. The main difference to the previous scenarios is a lower sensitivity of the concentration values to the calculated irrigation coefficient profile, and hence lower values of Q . Nonetheless, good fits to the true concentration and irrigation coefficient profiles are still obtained (Fig. 3C,G). The lower sensitivity, particularly in the upper centimeters of sediment, reflects the fact that nonzero rates increase the difference between the flushing concentration and the pore water concentration, which, in turn, facilitates identification of the true bioirrigation coefficient profile.

For the simulation results shown in Fig. 3D,H, a bioirrigation profile with a step function depth dependence was imposed. This corresponds qualitatively to the irrigation regime resulting from the activity of certain polychaetes (e.g., Craig and Lopez 1996). The model results fit the imposed profile extremely well, giving rise to values of Q that are generally much higher than in simulations for which a steeply decreasing bioirrigation coefficient profile was used. Thus, the inverse approach appears to be capable of identifying regions of markedly different irrigation intensities within the sediment column.

To illustrate spatial correlation, α values were interpolated linearly from the values at the center of the depth segments to the depths of the interface of two adjacent boxes. The oscillating values in the enveloping minimum and maximum of α values (Fig. 3A–D) reflect spatial coupling in the underlying individual profiles. These profiles, which are also consistent with the data available and their uncertainties, are ranked low in the statistical comparison because of the larger number of fitting parameters.

Model application

The inverse model was used to quantify bioirrigation coefficient values with depth in a variety of marine environments using measured data for three different chemical constituents (Table 1). Diffusion coefficients were either calculated as a function of temperature, salinity, and pressure and corrected for tortuosity (Ullman and Aller 1982), or they were taken directly from the studies to which our model results are compared. Pore water advection through the bulk sediment was neglected, whereas rapid, preferential flow through burrows was accounted for by the bioirrigation coefficient. The advective transport due to sedimentation was also neglected, because at all study sites, sedimentation rates are less than 10 mm yr^{-1} (Howarth and Giblin 1983; Christensen et al. 1984; Tromp et al. 1995, Glud et al. 1998), which is insignificant compared to diffusion and bioirrigation rates. Measured porosity, concentration and rate profiles were interpolated to the depths of the grid points using a weighted distance relationship. Input data resolution was set to 1 cm. For the Rn/Ra disequilibrium data, the reaction term included a first-order term accounting for the decay of pore water Rn, whereas the production of Rn through decay of Ra was accounted for using a zero-order rate based on the measured Rn secular equilibrium activity ($\lambda_{\text{Rn}} \phi \text{Rn}_{\text{porewater}}$ and $\lambda_{\text{Rn}} \phi \text{Rn}_{\text{equilibrium}}$, respectively, with λ_{Rn} being the ^{222}Rn decay constant of 3.824 d^{-1}). Constraints were applied to exclude negative values of the irrigation coefficients and calculated concentrations.

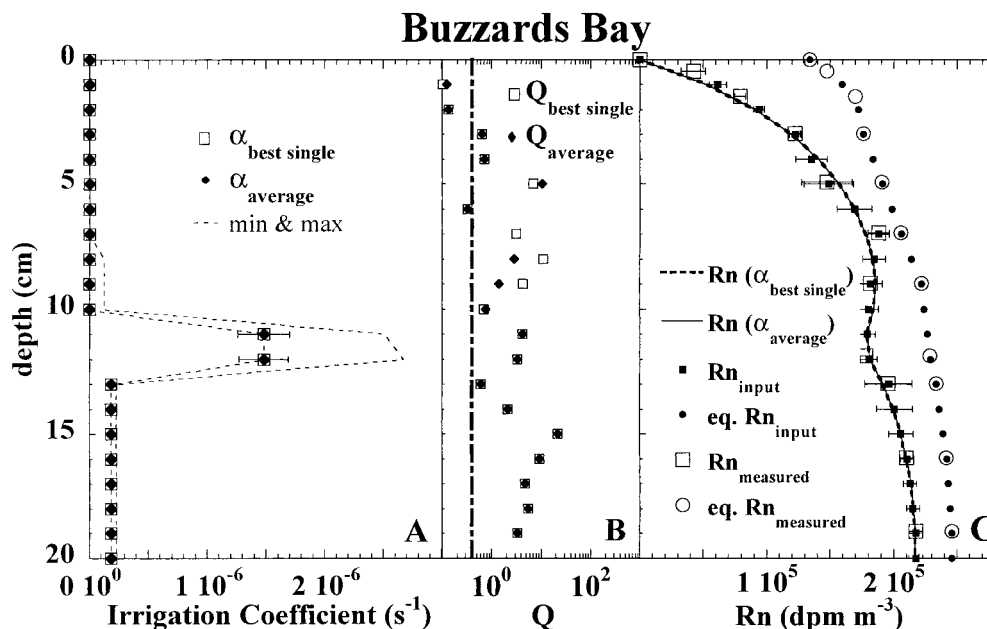


Fig. 4. Bioirrigation at Buzzards Bay. (A) The single, statistically best irrigation coefficient profile and the averaged irrigation coefficient profile, together with maximum and minimum values of the profiles with the least number of nonconverged boxes. (B) Quality function profile for the single, statistically best solution and the averaged solution. The dashed line shows the limit value of $Q = 0.4$. (C) Measured, interpolated, and calculated Rn pore water activities, as well as measured and interpolated secular equilibrium activity of Rn.

Subtidal estuary, Buzzards Bay, Massachusetts— $^{222}\text{Rn}/^{226}\text{Ra}$ disequilibrium has been used to study mixing processes in sediments (e.g., Hammond et al. 1977; Key et al. 1979; Gruebel and Martens 1984). Because of the large difference in the half-lives of parent and daughter isotope, any deviation of the measured Rn activity at a given depth in the sediment from its value at secular equilibrium may be attributed to transport processes. Martin and Banta (1992) used Rn/Ra disequilibrium data to quantify bioirrigation at a subtidal estuarine site at Buzzards Bay (Table 1). Bioirrigation coefficients calculated using the inverse model developed in this study could be directly compared to those of Martin and Banta (1992).

To apply the inverse model, Rn activities, porosity, and diffusivity data were taken directly from Martin and Banta (1992, see fig. 2, table 2). As in the latter study, it was assumed that the activity of Rn in the overlying water equals 0 and that the Rn profile represents steady state conditions. However, unlike in Martin and Banta's study, the lower boundary condition was set to a fixed Rn value, instead of applying an open system condition.

In agreement with Martin and Banta (1992), inverse model results indicate that solute transport in the top 5 cm of the sediment is dominated by diffusion, whereas below 5 cm depth both studies suggest that transport via bioirrigation is substantial compared to transport via diffusion. In addition, the depth-integrated value of α obtained with the inverse model (Table 1), which can be interpreted as a transfer velocity across the sediment-water interface and gives a measure for the overall intensity of bioirrigation at a given site, differs by less than a factor of two from Martin and Banta

(1992). However, in the upper diffusion-dominated portion of the sediment, values of Q are quite low (Fig. 4B), indicating that bioirrigation coefficients in this portion of the profile are not well constrained.

Although the depth-integrated irrigation coefficients found in the two studies are similar, the depth dependence of the irrigation coefficient obtained by the inverse method is quite different from that presented by Martin and Banta (1992). This is because Martin and Banta (1992) imposed an exponential shape of the irrigation coefficient profile in order to fit the measured Rn profile. With the inverse model, no a priori shape of the irrigation coefficient is assumed. According to the results of the inverse model, the irrigation coefficient exhibits a distinct subsurface maximum between 10 and 14 cm of sediment depth, rather than a monotonic change with depth (Fig. 4A). Such a subsurface maximum in the bioirrigation coefficient profile could reflect the activity of deposit feeders such as *Nephtys*, which have been reported by Martin and Banta (1992) at the study site. The same authors also observed a subsurface maximum in an excess bromide profile in one of the cores collected at the site.

Washington continental shelf—Bioirrigation has been quantified previously on the Washington Shelf using forward calculations based on Rn/Ra disequilibrium data and sulfate concentration plus reduction rate data (Smethie et al. 1981; Christensen et al. 1984). Bioirrigation coefficient profiles were calculated in this study by applying the inverse model to two sites on the Washington Shelf (Table 1) based on

Washington Shelf, core 2A

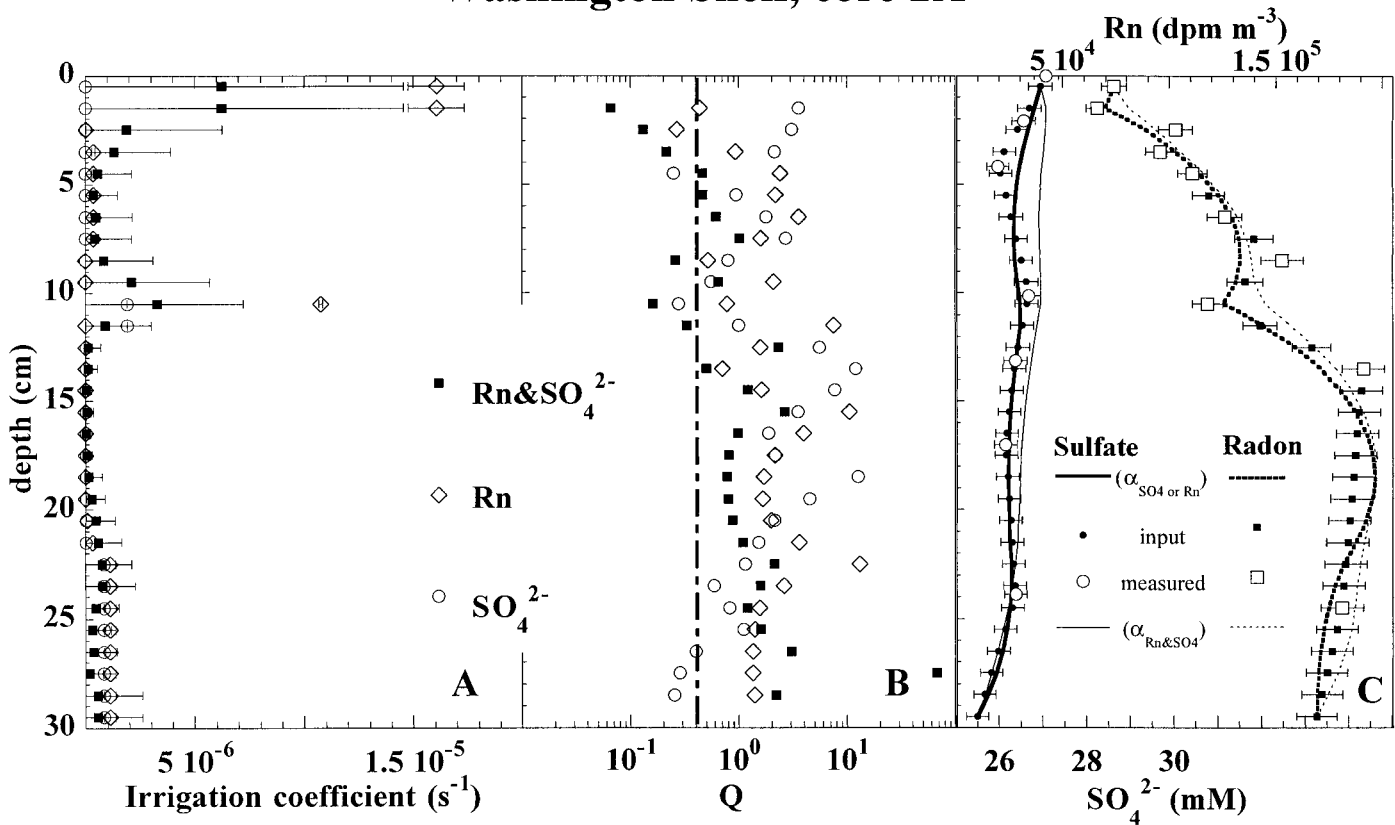


Fig. 5. Bioirrigation on the Washington Shelf, core 2A. (A) Average bioirrigation coefficient profile and (B) quality function obtained from simulations using Rn and sulfate data alone, as well as simultaneous optimization, respectively. (C) Calculated and measured sulfate concentrations and pore water radon activities, respectively. Sulfate reduction rates and Rn equilibrium activities used in these simulations (not shown) are from Christensen et al. (1984, fig. 2) and Smethie et al. (1981, table 1).

sulfate and Rn data alone, as well as from simultaneous optimization of both data sets.

Inverse model results obtained using either Rn or SO₄²⁻ profiles alone or both species simultaneously indicate significant bioirrigation to a depth of approximately 30 cm at both sites and high irrigation coefficients in core 3A near the sediment–water interface (Figs. 5A, 6A). The main difference in the bioirrigation profiles for the individual species occurs near the sediment–water interface in core 2A, where results obtained using the sulfate profiles alone give no indication of the intense irrigation suggested by the Rn profile (Fig. 5A). The results obtained for cores 2A and 3A using Rn, sulfate, or both suggest a subsurface maximum in irrigation at depths of approximately 11 and 19 cm, respectively (Figs. 5A, 6A).

From the difference in Rn and SO₄²⁻ diffusion coefficients, it might be expected that the bioirrigation coefficient values obtained from Rn data should be higher than those obtained using SO₄²⁻ data, possibly by as much as a factor of two. Such a difference in the magnitude of the irrigation coefficients is observed for the lower portion of core 2A, but not for core 3A. The lack of a systematic difference in bioirrigation coefficients between the two species justifies the simultaneous optimization of Rn and SO₄²⁻ profiles. In core 3A, simultaneous optimization of sulfate and Rn profiles

shows high values of α near the sediment–water interface and significant irrigation down to 30 cm deep, as found from the sulfate and Rn profiles alone (Fig. 6A). The multicomponent optimization in core 2A leads, not surprisingly, to intermediate values of α near the water–sediment interface, compared to the two single-species analyses, but the visually poor fit to the sulfate concentration as well as the low values of Q indicate the relatively low reliability of the model results in the upper few centimeters (Fig. 5B,C). It is difficult to determine the coefficients precisely over a large portion of the profile, as indicated by the large error bars associated with the irrigation coefficient profile. Nonetheless, it appears that the irrigation coefficients are relatively high near the top and bottom of the cores at both sites. Overall, the results obtained for both sites diverge significantly from the exponential decrease of α , which is often assumed in early diagenetic models (Martin and Sayles 1987; Wang and Van Cappellen 1996; Schlüter et al. 2000).

The inverse model results compare favorably to the findings of Christensen et al. (1984), who also found significant irrigation to a depth of 30 cm. However, Christensen et al. (1984) suggested the presence of a subsurface maximum in the bioirrigation coefficient at about 5 cm based on the SO₄²⁻ profiles. Such a subsurface maximum was not ob-

Washington Shelf, core 3A

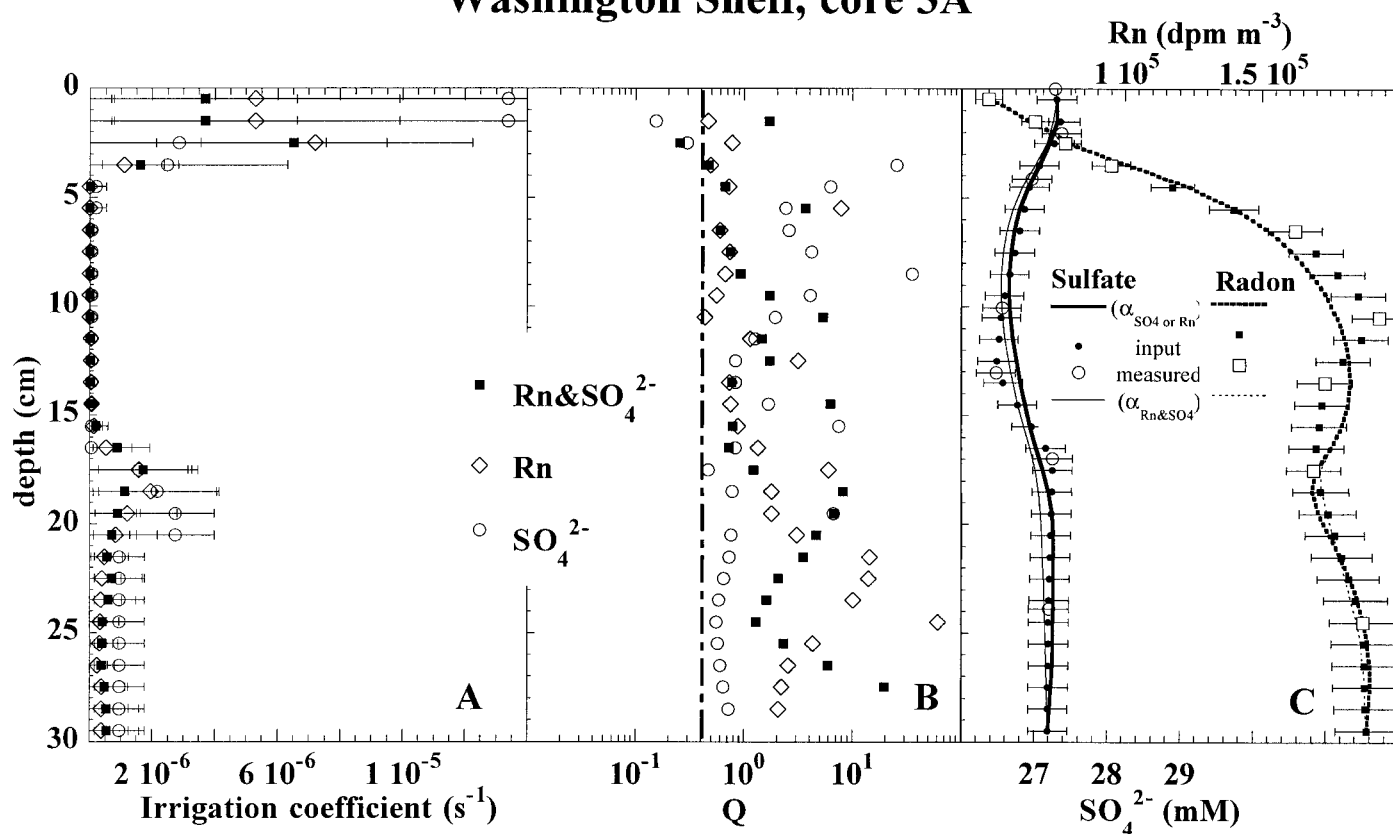


Fig. 6. Bioirrigation on the Washington Shelf, core 3A. Symbols and panels are the same as in Fig. 5. Sulfate reduction rates and Rn equilibrium activities used in these simulations (not shown) are from Christensen et al. (1984, fig. 2) and Smethie et al. (1981, table 1).

served in any of the profiles calculated here using the inverse model.

Independent evidence supports the validity of the bioirrigation profiles calculated by the inverse model, at least with respect to depth dependence. The subsurface maximum in the irrigation coefficients found in core 2A between 10 and 11 cm using the inverse method matches the depth of a worm burrow reported in core 2A by Smethie et al. (1981). This subsurface peak is apparent in profiles calculated with the inverse model using the sulfate or Rn data alone or using a combination of the two (Fig. 5), but it is not apparent in any of the calculated profiles reported by Christensen et al. (1984).

The deep, rapid solute transport implied by the high bioirrigation coefficients found near the bottom of the cores also helps to explain the observed departure of measured pore water Rn activities from secular equilibrium values. Smethie et al. (1981) attributed this difference to analytical overestimation of the equilibrium Rn activity. However, model simulations using corrected equilibrium activities proposed by Smethie et al. (1981) fail to produce enhanced bioirrigation coefficients at the depth of the reported burrow. This suggests that the difference in Rn activities may not be due to analytical artifacts, but rather to solute transport induced by deep, intense bioirrigation.

To further evaluate the bioirrigation coefficients predicted

by the inverse model, O_2 irrigation fluxes across the sediment–water interface at the Washington Shelf sites were estimated, assuming that the bioirrigation coefficients derived from the sulfate and Rn data apply to O_2 . If this assumption is violated, the calculated O_2 irrigation fluxes will tend to be underestimated because the high reactivity of O_2 would give rise to steep concentration gradients, which would accelerate diffusional transport of O_2 across burrow walls (Marinelli and Boudreau 1996). To calculate the O_2 irrigation fluxes, the sediment O_2 concentration was assumed to be negligible, and the O_2 flushing concentration was set to $130 \mu\text{M}$, as cited by Christensen et al. (1984). This leads to calculated irrigation fluxes of 2 ± 1.0 and $1.6 \pm 0.4 \text{ mmol } O_2 \text{ m}^{-2} \text{ d}^{-1}$ at sites MSSD-1 and -2, respectively, which is similar to the values of 1.2 and $2.5 \text{ mmol } O_2 \text{ m}^{-2} \text{ d}^{-1}$, respectively, calculated by Christensen et al. (1984). Archer and Devol (1992) determined O_2 irrigation fluxes on the Washington Shelf from the difference between total solute fluxes measured with benthic chambers and diffusive fluxes calculated from high-resolution pore water O_2 profiles. The O_2 irrigation fluxes reported by these authors near the study area ranged from 1.4 to $6.3 \text{ mmol m}^{-2} \text{ d}^{-1}$, which is of the same order of magnitude as the fluxes calculated using the inverse model results.

Arctic environment, Svalbard, Norway—Bioirrigation coefficient profiles were calculated for two sites near Svalbard,

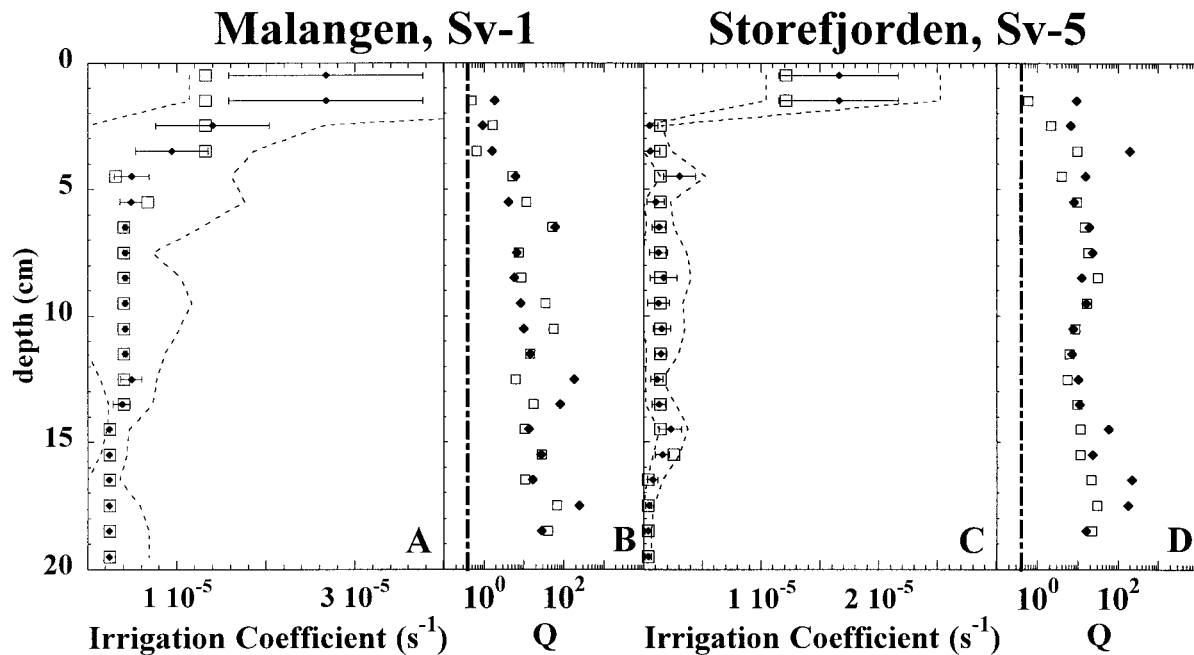


Fig. 7. Bioirrigation in the Svalbard region, based on DIC, R_{CO_2} , and pH profiles. Symbols and panels in (A) and (C), and (B) and (D) are the same as in Fig. 4A,B, respectively. DIC concentrations and DIC production rates used in these simulations (not shown) are from Kostka et al. (1999, figs. 2, 6).

Norway; one at Malangen Fjord and the other at Storefjorden (Sv-1 and Sv-5, respectively, Table 1). The bioirrigation profiles were optimized using profiles of dissolved inorganic carbon (DIC) concentration, DIC production rate (R_{CO_2}) and pH for the two sites described in Kostka et al. (1999). The diffusion coefficient for DIC was calculated from the diffusivities of the different carbonate species, weighted according to their relative contribution to DIC based on the measured pH values.

Calculated bioirrigation coefficient profiles at both sites show very high depth-integrated values of α (Table 1) and a distinct decrease of α with depth (Fig. 7A,C). The quality function has high values over the entire profile (Fig. 7B,D), and the calculated concentrations are within the uncertainties of the interpolated measurements (not shown). This provides a high level of confidence that the calculated bioirrigation coefficient profiles are meaningful and implies a very active benthic macrofauna in these Arctic environments.

To assess the inverse model results, calculated O_2 irrigation fluxes were compared to the difference between measured benthic oxygen fluxes and diffusive fluxes calculated from O_2 microelectrode profiles measured at the Storefjorden site (Glud et al. 1998). Irrigation fluxes were calculated using the measured bottom water O_2 concentration of $328 \mu\text{M}$ as the flushing concentration, and because the O_2 penetration depth is approximately 1 cm and the concentration decreases approximately linearly with depth (Glud et al. 1998), the O_2 concentration was assumed to be half the flushing concentration in the top centimeter of sediment and 0 below. This calculation results in an estimated irrigation flux of approximately $10 \text{ mmol O}_2 \text{ m}^{-2} \text{ d}^{-1}$, which is 2.5 times greater than the difference between the measured benthic and diffusive fluxes of $3.9 \pm 1.5 \text{ mmol O}_2 \text{ m}^{-2} \text{ d}^{-1}$. The irrigation flux of

DIC calculated from the irrigation coefficient profile also exceeds the difference between measured benthic and diffusive fluxes (Glud et al. 1998) by about a factor of 2.5. At present, the reason for the discrepancy between calculated and measured irrigation fluxes is unclear.

Salt marsh environment, Sapelo Island, Georgia—Salt marsh sediments are densely populated by macrofauna, including fiddler crabs, mud crabs, polychaete worms, and shrimp, all of which may build extensive burrow networks (e.g., Teal 1958; Basan and Frey 1977). Therefore, bioirrigation is likely to be an important solute transport process in salt marsh sediments. Nonetheless, few attempts have been made to quantify bioirrigation in these environments. Here, the inverse model was applied to data collected at an unvegetated creek bank site at Sapelo Island, a barrier island $\sim 8 \text{ km}$ off the coast of Georgia (Table 1).

Sulfate concentrations were measured on pore waters collected using diffusion equilibrators (Koretsky et al. in prep.), and sulfate reduction rates were determined by adding trace quantities of $^{35}\text{SO}_4^{2-}$ to sediments (Jørgensen 1978) and incubating them for 2 h (Kostka et al. pers. comm.). To derive irrigation coefficients using the inverse model, net rates of sulfate consumption are required. Thus, if in situ reoxidation of reduced sulfur is significantly higher than during the 2-h laboratory incubation, this would lead to an overestimation of the calculated irrigation coefficients. This might occur, for example, because O_2 is entirely excluded in the laboratory experiment, whereas in the field O_2 may be introduced into the sediment via bioirrigation.

Calculated irrigation profiles might also be biased because sulfate concentration profiles measured using diffusion equilibrators represent pore water concentrations averaged

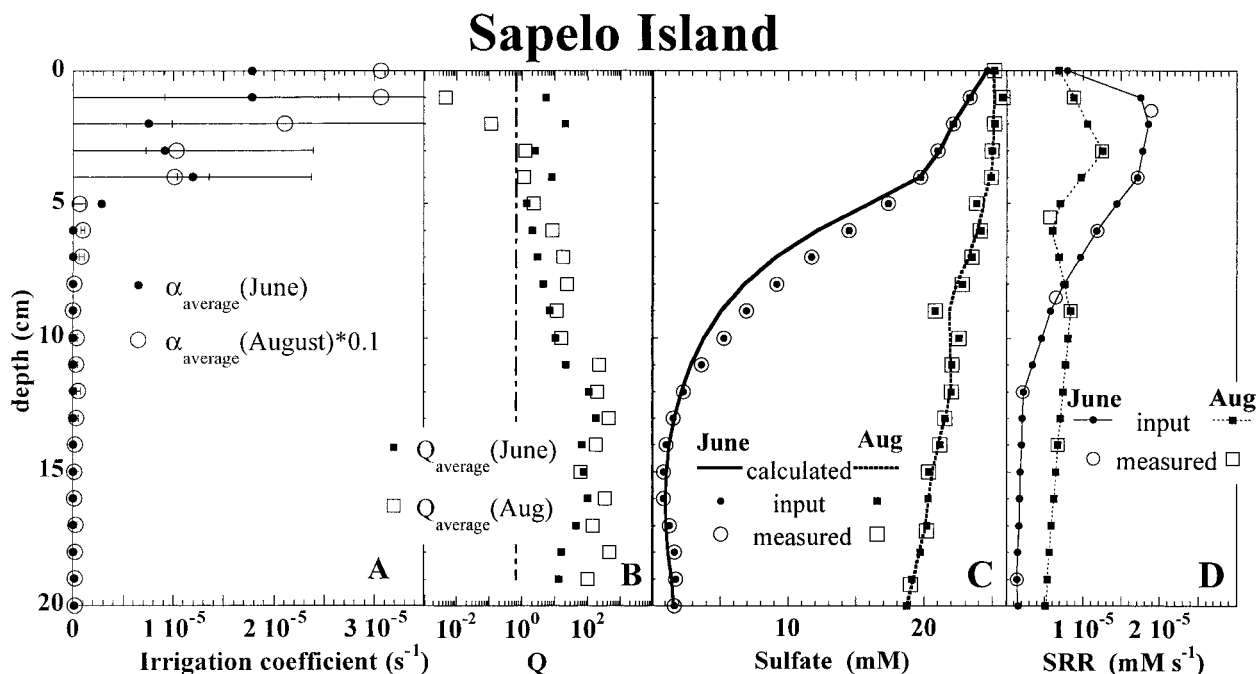


Fig. 8. Bioirrigation at Sapelo Island in June 1998 and August 1997, based on sulfate profiles and sulfate reduction rates (Koretsky et al. in prep.).

over several days to weeks, whereas the sulfate reduction rates represent instantaneous rates. This difference in time-scales may influence model results significantly if the sulfate pore water concentrations, sulfate flushing concentrations, or sulfate reduction rates fluctuated greatly during the 3-week deployment period of the diffusion equilibrators. Furthermore, the time resolution of the concentration and reduction rate data do not allow potential nonsteady state effects on the measured profiles to be addressed. Thus, the data were assumed to represent seasonal quasi-steady states, in spite of the fact that salt marshes are clearly dynamic ecosystems.

The bioirrigation coefficients calculated from the sulfate concentration and reduction rate profiles are high in the uppermost 5 cm of the sediment column, both for June and August (Fig. 8A). However, low values of Q in August near the sediment–water interface indicate that the bioirrigation coefficients are not well constrained (Fig. 8B). This is because the sulfate flushing concentration lies within the uncertainty interval of the measured sulfate concentrations near the sediment–water interface (Fig. 8C). Thus, the irrigation coefficient is likely to be overpredicted in the uppermost 4 cm.

As for the Svalbard and Washington Shelf sites, the O_2 irrigation flux across the sediment–water interface was calculated using the bioirrigation coefficient profiles. To calculate the O_2 flux due to irrigation, the bulk sediment was assumed to have negligible O_2 concentrations at all depths. O_2 flushing concentrations of 211 μM in June and 193 μM in August were set by assuming saturation with respect to atmospheric O_2 (at 25 and 30°C, Kostka et al. pers. comm.). These assumptions, combined with the calculated bioirrigation coefficient profiles, yield estimated bioirrigation O_2 flux-

es of 8.1 ± 1.1 and $117 \pm 115 \text{ mmol } O_2 \text{ m}^{-2} \text{ d}^{-1}$ in June and August, respectively.

Oxygen uptake by a salt marsh sediment at Sapelo Island was estimated by Teal and Kanwisher (1961) to be approximately $17 \text{ mmol m}^{-2} \text{ d}^{-1}$, but their data do not allow the relative contribution of diffusion to the total flux to be calculated. The overall O_2 benthic flux reported by Teal and Kanwisher (1961) and the calculated O_2 irrigation flux for June from this study are at least qualitatively consistent, but the measured O_2 benthic flux suggests that the irrigation flux calculated here for August is too high. The implication that the August irrigation coefficients are overestimated is perhaps not surprising, given the low values of Q and the large error bars associated with the extremely high irrigation coefficients calculated near the sediment–water interface.

Results of this study support previous findings that sulfate reduction rates cannot always be inferred directly from sulfate concentration gradients in heavily bioturbated sediments (e.g., Berner 1985; Fossing et al. 2000; Furukawa et al. 2000). In addition, the high irrigation intensities found for the Sapelo Island sediment imply that biologically induced transport efficiently counters sulfate depletion and thereby helps sustain high sulfate reduction rates. Thus, intense macrofaunal activity, by supporting high fluxes of sulfate and O_2 , helps explain low emissions of methane from highly productive salt marshes (Howarth and Giblin 1983).

Conclusions

In many natural sediments, the quality and quantity of available data are such that many different bioirrigation coefficient profiles can fit measured data within the limits of

uncertainty. Therefore, it may not be possible to uniquely determine the true irrigation coefficient profiles. Nonetheless, as shown here, it is possible to rank potential solutions according to objective criteria and to judge the meaningfulness of results using algorithms such as the quality function developed in this study. The proposed quality function reflects both the sensitivity of concentration profiles to changes in the bioirrigation coefficient and the goodness of the fit between calculated and measured concentration profiles.

The inverse model was used in this study to calculate bioirrigation coefficient profiles in four different marine sedimentary environments. The model results indicate the existence of subsurface maxima in bioirrigation intensity at sites in Buzzards Bay and on the Washington Shelf. Previous studies failed to reveal these features at these sites. The model results highlight one of the primary advantages of using the inverse approach; namely, that it does not require an a priori, and therefore biased, definition of the depth dependence of the irrigation coefficient.

Bioirrigation coefficient profiles obtained with the inverse model were used to estimate irrigation O₂ fluxes across the sediment–water interface. These estimates were compared to irrigation fluxes derived from the difference between measured benthic and calculated diffusive fluxes at sites with available data. In most cases, the O₂ fluxes estimated from the calculated irrigation coefficient profiles were of the same order of magnitude as measured fluxes. The worst agreement was found between measured and calculated irrigation fluxes for the August data from the Sapelo Island salt marsh site. However, the calculated irrigation coefficient profile was also characterized by very low values of the quality function. Thus, the poor reliability of the calculated irrigation coefficients would have been established even without comparison to an independent data set.

The inclusion of nonlocal solute transport in early diagenetic reactive transport models (e.g., Boudreau 1996; Wang and Van Cappellen 1996) creates the need for an objective parameterization of bioirrigation coefficients. The model presented provides a new tool for the unbiased interpretation of data collected in a variety of aquatic sediments. The model is available, compiled for Macintosh PowerPCs by contacting the first author (meile@geo.uu.nl). It can be used not only to determine bioirrigation coefficient profiles, but also to determine reaction rate profiles (i.e., zones of consumption or production) for environments in which transport processes are known.

References

- ALLER, R. C. 1980. Quantifying solute distributions in the bioturbated zone of marine sediments by defining an average micro-environment. *Geochim. Cosmochim. Acta* **44**: 1955–1965.
- , AND J. Y. ALLER. 1998. The effect of biogenic irrigation intensity and solute exchange on diagenetic reaction rates in marine sediments. *J. Mar. Res.* **56**: 905–936.
- , J. Y. YINGST, AND W. J. ULLMAN. 1983. Comparative biogeochemistry of water in intertidal *Onuphis* (polychaeta) and *Upogebia* (crustacea) burrows: Temporal patterns and causes. *J. Mar. Res.* **41**: 571–604.
- ARCHER, D., AND A. DEVOL. 1992. Benthic oxygen fluxes on the Washington shelf and slope: A comparison of in situ micro-electrode and chamber flux measurements. *Limnol. Oceanogr.* **37**: 614–629.
- BASAN, P. B., AND R. W. FREY. 1977. Actual-palaeontology and neoichnology of salt marshes near Sapelo Island, Georgia, p.41–70. *In* T. P. Crimes and J. C. Harper [eds.], *Trace fossils* 2. Steel House Press.
- BERG, P., N. RISGAARD-PETERSEN, AND S. RYSGAARD. 1998. Interpretation of measured concentration profiles in sediment pore water. *Limnol. Oceanogr.* **43**: 1500–1510.
- BERNER, R. A. 1985. Sulphate reduction, organic matter decomposition and pyrite formation. *Phil. Trans. R. Soc. Lond., A* **315**: 25–38.
- BOUDREAU, B. P. 1984. On the equivalence of nonlocal and radial-diffusion models for porewater irrigation. *J. Mar. Res.* **42**: 731–735.
- . 1987. Mathematics of tracer mixing in sediments. III. The theory of nonlocal mixing within sediments. *Am. J. Sci.* **287**: 693–719.
- . 1996. A method-of-lines code for carbon and nutrient diagenesis in aquatic sediments. *Computers Geosci.* **22**: 479–496.
- . 1997. *Diagenetic models and their implementation*. Springer.
- CHRISTENSEN, J. P., A. H. DEVOL, AND W. M. SMETHIE. 1984. Biological enhancement of solute exchange between sediments and bottom water on the Washington continental shelf. *Continental Shelf Res.* **3**: 9–23.
- CRAIG, N. I., AND G. R. LOPEZ. 1996. Reactive and nonreactive particle dynamics in dense assemblages of the head down deposit feeder *Clymenella torquata*, p.30. *In* S. A. Woodin and others [eds.], *24th Annual Benthic Ecology Meeting*, Columbia, South Carolina, March 7–10, 1996.
- EMERSON, S., R. JAHNKE, AND D. HEGGIE. 1984. Sediment–water exchange in shallow water estuarine sediments. *J. Mar. Res.* **42**: 709–730.
- FIADDEIRO, M. E., AND G. VERONIS. 1977. On weighted-mean schemes for the finite-difference approximation to the advection-diffusion equation. *Tellus* **29**: 512–522.
- FOSSING, H., T. G. FERDELMAN, AND P. BERG. 2000. Sulfate reduction and methane oxidation in continental margin sediments influenced by irrigation (South-East Atlantic off Namibia). *Geochim. Cosmochim. Acta* **64**: 897–910.
- FURUKAWA, Y., S. BENTLEY, A. SHILLER, D. LAVOIE, AND P. VAN CAPPELLEN. 2000. The role of biologically-enhanced pore water transport in early diagenesis: An example from carbonate sediments in the vicinity of North Key Harbor, Dry Tortugas National Park, Florida. *J. Mar. Res.* **58**: 493–522.
- GLUD, R. N., O. HOLBY, F. HOFFMANN, AND D. CANFIELD. 1998. Benthic mineralisation and exchange in Arctic sediments (Svalbard, Norway). *Mar. Ecol. Prog. Ser.* **173**: 237–251.
- GRUEBEL, K. A., AND C. S. MARTENS. 1984. Radon-222 tracing of sediment–water chemical transport in an estuarine sediment. *Limnol. Oceanogr.* **29**: 587–597.
- HAMMOND, D. E., AND C. FULLER. 1979. The use of Radon-222 to estimate benthic exchange and atmospheric exchanges in San Francisco Bay, p.213–230. *In* T. J. Conomos [ed.], *San Francisco Bay, the urbanized estuary*. American Association for the Advancement of Science.
- , H. J. SIMPSON, AND G. MATHIEU. 1977. Radon-222 distribution and transport across the sediment–water interface in the Hudson River estuary. *J. Geophys. Res.* **82**: 3913–3920.
- , AND OTHERS. 1985. Benthic fluxes in San Francisco Bay. *Hydrobiologia* **129**: 69–90.
- HOWARTH, R. W., AND A. GIBLIN. 1983. Sulfate reduction in the salt marshes at Sapelo Island, Ga. *Limnol. Oceanogr.* **28**: 70–82.
- JØRGENSEN, B. B. 1978. A comparison of methods for the quanti-

- fication of bacterial sulfate reduction in coastal marine sediments. I. Measurement with radiotracer methods. *Geomicrobiology* **1**: 11–27.
- KEY, R. M., N. L. J. GUINASSO, AND D. R. SCHINK. 1979. Emanation of radon-222 from marine sediments. *Mar. Chem.* **7**: 221–250.
- KLEINBAUM, D. G., L. L. KUPPER, AND K. E. MULLER. 1988. Applied regression analysis and other multivariate methods, 2nd ed. PWS-KENT.
- KOSTKA, J. E., B. THAMDRUP, R. N. GLUD, AND D. E. CANFIELD. 1999. Rates and pathways of carbon oxidation in permanently cold arctic sediments. *Mar. Ecol. Prog. Ser.* **180**: 7–21.
- LOWE, K. L., T. J. DICHRISTINA, A. ROYCHODHURY, AND P. VAN CAPPELLEN. 2000. Microbiological and geochemical characterization of microbial Fe(III) reduction in salt marsh sediments. *Geomicrobiol. J.* **17**: 163–178.
- MARINELLI, R. L., AND B. P. BOUDREAU. 1996. An experimental and modeling study of pH and related solutes in an irrigated anoxic coastal sediment. *J. Mar. Res.* **54**: 939–966.
- MARTIN, W. R., AND G. T. BANTA. 1992. The measurement of sediment irrigation rates: A comparison of the Br⁻ tracer and ²²²Rn/²²⁶Ra disequilibrium techniques. *J. Mar. Res.* **50**: 125–154.
- , AND F. L. SAYLES. 1987. Seasonal cycles of particle and solute transport processes in nearshore sediments: ²²²Rn/²²⁶Ra and ²³⁴Th/²³⁸U disequilibrium at a site in Buzzards Bay, MA. *Geochim. Cosmochim. Acta* **51**: 927–943.
- MAYER, M. S., L. SCHAFFNER, AND W. M. KEMP. 1995. Nitrification potentials of benthic macrofaunal tubes and burrow walls: Effects of sediment NH₄⁺ and animal irrigation behavior. *Mar. Ecol. Prog. Ser.* **121**: 157–169.
- MEILE, C. 1999. An inverse model for reactive transport in biogeochemical systems: Application to biologically-enhanced pore water transport (irrigation) in aquatic sediments. M.Sc. thesis, Georgia Institute of Technology.
- PRESS, W. H., B. P. FLANNERY, S. A. TEUKOLSKY, AND W. T. VETTERLING. 1989. Numerical recipes (Fortran version). Cambridge University Press.
- ROWE, G. T., C. H. CLIFFORD, K. L. J. SMITH, AND P. L. HAMILTON. 1975. Benthic nutrient regeneration and its coupling to primary production in coastal waters. *Nature* **255**: 215–217.
- SCHLÜTER, M., E. SAUTER, H.-P. HANSEN, AND E. SUESS. 2000. Seasonal variations of bioirrigation in coastal sediments: Modelling of field data. *Geochim. Cosmochim. Acta* **64**: 821–834.
- SMETHIE, W. M. J., C. A. NITTROUER, AND R. F. L. SELF. 1981. The use of radon-222 as a tracer of sediment irrigation and mixing on the Washington continental shelf. *Mar. Geol.* **42**: 173–200.
- TEAL, J. M. 1958. Distribution of fiddler crabs in Georgia salt marshes. *Ecology* **39**: 185–193.
- , AND J. KANWISHER. 1961. Gas exchange in a Georgia salt marsh. *Limnol. Oceanogr.* **6**: 388–399.
- TROMP, T. K., P. VAN CAPPELLEN, AND R. M. KEY. 1995. A global model for the early diagenesis of organic carbon and organic phosphorus in marine sediments. *Geochim. Cosmochim. Acta* **59**: 1259–1284.
- ULLMAN, W. J., AND R. C. ALLER. 1982. Diffusion coefficients in nearshore marine sediments. *Limnol. Oceanogr.* **27**: 552–556.
- WANG, Y., AND P. VAN CAPPELLEN. 1996. A multicomponent reactive transport model of early diagenesis: Application to redox cycling in coastal marine sediments. *Geochim. Cosmochim. Acta* **60**: 2993–3014.

Received: 13 April 2000

Accepted: 28 August 2000

Amended: 12 September 2000